**TECHNICAL TRANSACTIONS** | **CZASOPISMO TECHNICZNE**
ELECTRICAL ENGINEERING | ELEKTROTECHNIKA
1-E/2015

PIOTR BOGUSZ*

# INFLUENCE OF CONTROL PARAMETERS ON PROPERTIES OF THE HIGH SPEED TWO-PHASE SWITCHED RELUCTANCE DRIVE

# WPŁYW PARAMETRÓW STEROWANIA NA WŁAŚCIWOŚCI WYSOKOOBROTOWEGO NAPĘDU Z DWUPASMOWYM SILNIKIEM RELUKTANCYJNYM PRZEŁĄCZALNYM

Abstract

Two-phase switched reluctance motors are distinguished by their very simple design and belong to the group of high-speed motors. At high rotational speeds, losses in the core of a 4/2-pole switched reluctance machine are much lower than those occurring in a SRM with a larger number of phases. Unfortunately, a flaw of such a solution consists of a difficulty to obtain the starting torque in certain rotor positions. This occurs in the case of a symmetrical stator and rotor layout. To obtain the starting torque in any rotor position, an asymmetric design of rotor has been employed. In the framework of this study, a simulation model of such a machine was developed with the use of which motor characteristics were obtained for two specific working points, namely for very low and very high rotor speeds. Special attention was also focused on the problem of voltage control at high rotor speeds. On the grounds of the obtained results, an analysis of properties of the examined drive was performed from the point of view of the development of a practical control circuit for a two-phase SRM.

*Keywords*: *high speed drive*, *switched reluctance motor*, *simulation model*

Streszczenie

Dwupasmowe silniki reluktancyjne przełączalne charakteryzują się bardzo prostą konstrukcją i należą do grupy silników wysokoobrotowych. Przy dużych prędkościach wirowania wirnika w maszynie SRM 4/2 w rdzeniu występują znacznie mniejsze straty w porównaniu do SRM o większej liczbie pasm. Niestety wadą tego rozwiązania jest problem z uzyskaniem w każdym położeniu wirnika momentu rozruchowego, tak jak w przypadku symetrycznej konstrukcji stojana i wirnika. Aby uzyskać moment rozruchowy w każdym położeniu, zastosowano niesymetryczną budowę wirnika. W ramach niniejszej pracy zbudowano model symulacyjny omawianej maszyny, za pomocą którego uzyskano wyniki badań dla dwóch przypadków pracy, tj. dla bardzo małych i bardzo dużych prędkości wirowania wirnika. Zwrócono również uwagę na problem regulacji napięcia przy dużych prędkościach wirnika. Na podstawie uzyskanych wyników przeprowadzono analizę właściwości tego napędu pod kątem opracowania praktycznego układu sterownika dla dwupasmowego silnika SRM.

*Słowa kluczowe*: *napęd wysokoobrotowy*, *silnik reluktancyjny przełączalny*, *model symulacyjny*

**DOI: 10.4467/2353737XCT.15.032.3832**

* D.Sc. Eng. Piotr Bogusz, Dept. of Electrodynamics and Electrical Machine Systems, Faculty of Electrical and Computer Engineering, Rzeszow University of Technology.

## 1. Introduction

In household appliances such as vacuum cleaners, juice extractors, and food processors, ac commutator motors are commonly used. Drives of this type have a number of flaws, including, among other things, the generation of electromagnetic interference, susceptibility to failures, and lower efficiency compared to brushless drives. An alternative solution allowing potentially to supplant commutator motors are switched reluctance machines (SRM) distinguished by their very simple construction, absence of commutators, absence of windings and permanent magnets on rotor. Additionally, motors of this type have very good properties including a wide range speed control and are characterized with a higher efficiency compared to commutator motors. Drives employing SRMs, in view of the simple design of their rotors, are very suitable for use in high-speed appliances [1–3]. Flaws of drives of this type include their relatively large torque pulsation and high noise levels relating to the pulsed supply of windings. Recently, a number of studies were published on high-speed drives with switched reluctance motors [2–7]. In general, high-speed SRM drives are constructed as two-phase 4/2-pole machines as such designs allow reducing the switching frequency and as a consequence, reduce losses in the motor core. Limiting the number of motor phases to two means a significant reduction of costs relating to control as less power transistors and diodes are required which represent the most costly items on the list of control system components. In high-speed drives designed, for example, for vacuum cleaner suction units where the motor operates in a single-channel mode, it is possible to use a two-phase SRM with an asymmetric rotor. A characteristic feature of such a solution is the possibility to produce torque in any rotor position, contrary to two-phase SRM designs with a symmetric rotor [3–5]. An important issue is the control method selected for such a motor. In paper [6], a specific technique for torque pulsation minimization at high rotor rotational speeds is proposed, while paper [7] discloses a solution for a SRM controller utilizing a signal processor.

The purpose of this paper is to present results obtained from simulations and preliminary laboratory tests of a two-phase 4/2-pole high-speed SRM with an asymmetric rotor. Simulations were aimed at the determination of the effect of control parameters on the performance of the drive. Knowledge of the control parameters allowed in turn to develop algorithms optimizing the performance of the drive at a specific design working point. The designed and constructed control module was based on a microprocessor circuit allowing for convenient implementation of the control algorithm.

## 2. Mathematical model

Neglecting eddy currents in the stator and rotor cores and assuming that in the case of non-linearity of the magnetic circuit, the associated flux vector $\boldsymbol{\psi}$ depends on the rotor position $\theta$ and on $N$ currents in individual machine winding phases $i_1, ..., i_N$ according to definition:

$$\boldsymbol{\psi}(\theta,\mathbf{i}) \stackrel{def}{=} \left[ \psi_1(\theta,i_1,...,i_N), ..., \psi_N(\theta,i_1,...,i_N) \right]^T, \tag{1}$$

equations describing a $N$-phase SRM can be written as follows:

$$\mathbf{u} = \mathbf{R}\,\mathbf{i} + \frac{\mathrm{d}}{\mathrm{d}t}\boldsymbol{\psi}(\theta, \mathbf{i}) \,, \tag{2}$$

$$J\frac{\mathrm{d}\omega}{\mathrm{d}t} + D\omega + T_L = T_e \,, \tag{3}$$

$$\frac{\mathrm{d}\theta}{\mathrm{d}t} = \omega \,, \tag{4}$$

$$T_e = \frac{\partial W_c^*(\theta, \mathbf{i})}{\partial \theta} \,, \tag{5}$$

where:
$\mathbf{u} = [u_1, ..., u_N]$,
$\mathbf{i} = [i_1, ..., i_N]$,
$\mathbf{R} = \mathrm{diag}[R_1, ..., R_N]$,
$\theta$ – the rotor position angle,
$\omega$ – rotor angular speed,
$J$ – rotor's moment of inertia,
$D$ – coefficient of viscous friction,
$T_L$ – load torque,
$T_e$ – motor electromagnetic torque,
$W_c^*(\theta, \mathbf{i})$ – total magnetic field co-energy in the machine's air gap.

## 3. Simulation model

The subject of simulation studies was the two-phase switched reluctance motor with stepper air gap of the rotor. The geometry of the motor is presented in Fig. 1. As the motor has an asymmetric structure, flux-current-angle and torque-current-angle characteristics for the full electric cycle were employed in the simulation model and calculated with the use of FEM. These characteristics for selected phase current values are presented in Fig. 2. As it follows from Fig. 2, the motor can produce a positive torque value within the rotor position range $0° \le \theta \le 110°$. As the motor is designed to be supplied directly from 230 V electric power grid, apart from the motor model and the controlled converter, a bridge rectifier was used. The simulation model was developed in the MATLAB/Simulink environment with the use of the SimPowerSystems library.


Fig. 1. Geometry of the 4/2 SRM: (a) stator, (b) rotor

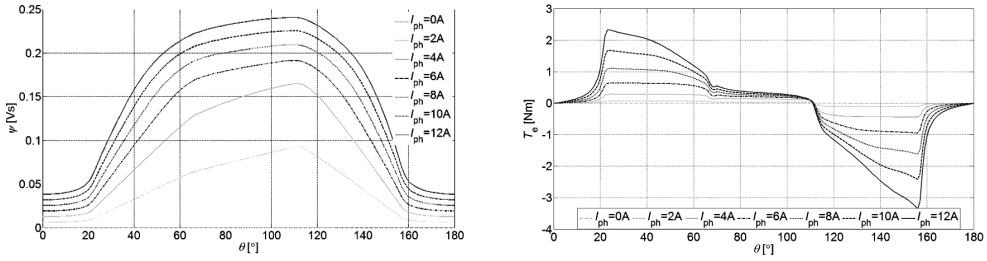


Fig. 2. Characteristics of a 4/2 SRM: a) $\psi = f(\theta)$, b) $T_e = f(\theta)$ for different values of current $i_{ph}$

Parameters of the examined motor are listed in Table 1.

Table 1

**Parameters of the examined SRM**

| | |
|---|---|
| Number of stator teeth, *Ns* | 4 |
| Number of rotor teeth, $N_r$ | 2 |
| Nominal voltage | 325 V dc |
| Nominal rotor speed, $n_N$ | 45 000 rpm |
| Nominal power, $P_N$ | 700 W |

A block diagram of the simulation model developed for the examined motor is presented in Fig. 3.

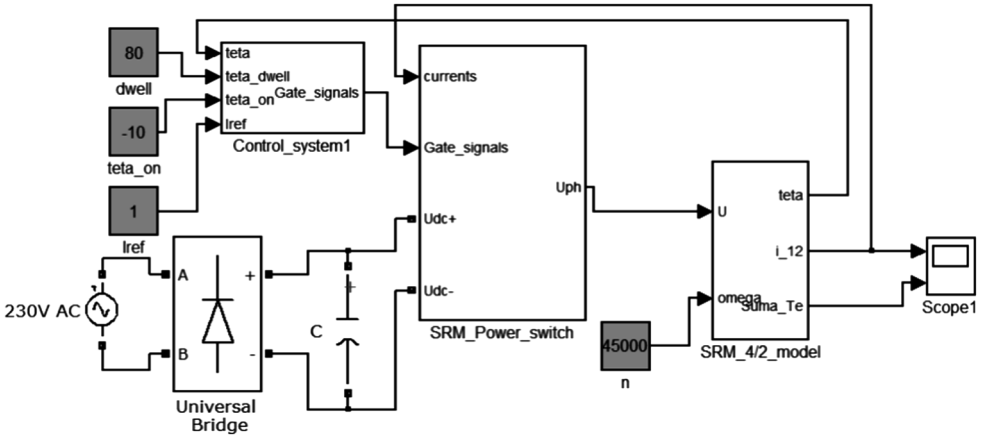


Fig. 3. A block diagram of SRM drive simulation model

The examined motor is designed to be used in a drive for vacuum cleaner suction where high starting torque is not necessary. The angle $\theta = 0°$ was selected as corresponding to the unaligned position of the rotor.

## 4. Simulation results

### 4.1. Static characteristics

#### 4.1.1. Supply range $\theta_{supply} = 90°$

Waveforms of the resultant motor torque with idealized square shapes of phase currents $i_{ph1}$ and $i_{ph2}$ for which the maximum value was adopted to be 6 A, for the supply range $\theta_{supply} = 90°$, and turn-on angles $\theta_{on} = 0°$ and 20°, are presented in Fig. 4. Comparing waveforms presented in Figs. 4a) and b), it can be observed that with windings supplied in such a way that $\theta_{on} = 0°$ and $\theta_{supply} = 90°$, there are points in which the starting torque equals 0. In cases where motor windings are supplied with a delay of 20° (counting from the unaligned position of the rotor), the minimum torque value is $T_{emin} = 0.1$ Nm. This means that a 20° turn-on delay results in a significant increase in the motor starting torque; moreover, the torque has a nonzero value in any position of the rotor.

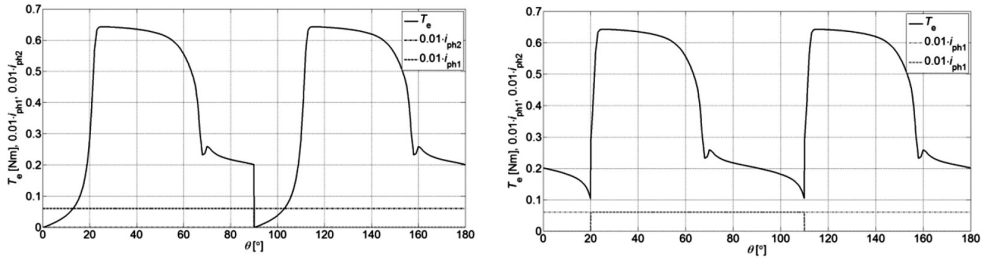


Fig. 4. Motor torque waveforms for the supply angle $\theta_{supply} = 90°$ and the turn-on angle: a) $\theta_{on} = 0°$, b) $\theta_{on} = 20°$

#### 4.1.2. Supply range $\theta_{supply} = 110°$

The examined motor achieves the largest starting torque when the turn-on angle is $\theta_{on} = 0°$, and the supply range $\theta_{supply} = 110°$.

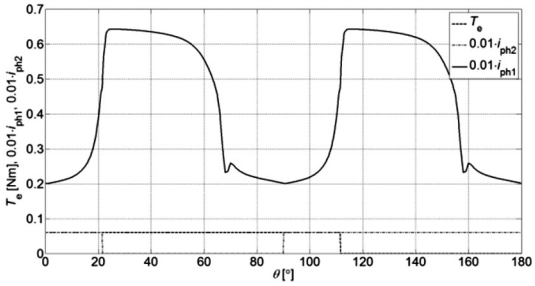


Fig. 5. The motor torque waveform for the supply range $\theta_{supply} = 110°$ and the turn-on angle $\theta_{on} = 0°$

For these parameters, the minimum torque value is $T_{emin}$ = 0.2 Nm. The torque waveform for this case is presented in Fig. 5. When $\theta_{supply}$ = 110° and $\theta_{on}$ = 0°, the minimum starting torque value is twice as high compared to the case $\theta_{supply}$ = 90° and $\theta_{on}$ = 20°.

## 4.2. Motor steady-state operation

### 4.2.1. Low-speed operation

Plots of the torque average value ($T_{eav}$), supply current ($I_{dcav}$), $T_{eav}/I_{dcav}$ ratio, and the torque minimum value ($T_{emin}$) as functions of the turn-on angle are shown in Fig. 6. The characteristics have been determined for motor speed $n$ = 100 rpm and different supply ranges ($\theta_{supply}$) that were changed within the interval from 90° to 110°, with phase currents limited to $I_{ref}$ = 6 A.

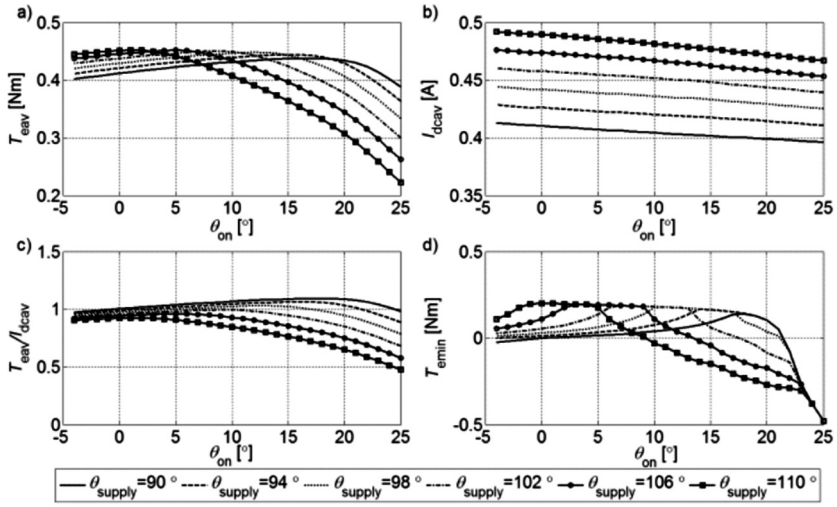


Fig. 6. Functional relationships for different supply ranges ($\theta_{supply}$): a) $T_{eav} = f(\theta_{on})$, b) $I_{dcav} = f(\theta_{on})$, c) $T_{eav}/I_{dcav} = f(\theta_{on})$, d) $T_{emin} = f(\theta_{on})$, at $n$ = 100 rpm; $I_{ref}$ = 6 A

It follows from Fig. 6a) that it is possible to maintain the average torque produced by the motor on the level $T_{eav}$ = 0.45 Nm, with phase current amplitude set to 6 A for various combinations of the turn-on angle and supply range values. A parameter very important for motor performance at starting is the minimum torque value $T_{emin}$, presented in Fig. 6d) as a function of the turn-on angle for different supply ranges. Delaying the winding turn-on position by angles larger than 20° results in a rapid decrease of the minimum torque value. The maximum $T_{eav}/I_{dcav}$ ratio occurs for the supply range $\theta_{supply}$ = 90° and the turn-on angle $\theta_{on}$ = 20° (Fig. 6c)). The supply current value $I_{dcav}$ as a function of the turn-on angle for different supply ranges is presented in Fig. 6b).

### 4.2.2. Nominal operating point

The examined motor is designed to operate at nominal speed $n_N$ = 45 000 rpm and output mechanical power $P_N$ = 700 W. To ensure an adequate amount of the produced torque with increasing speed, it is necessary to change the control position angles. This mainly follows from increase of back-EMF. Figure 7 shows waveforms of phase currents ($i_{ph1}$, $i_{ph2}$), phase torques ($T_{eph1}$, $T_{eph2}$), and the total electromagnetic current ($T_e$) of the motor determined under the following conditions: $U_{dc}$ = 325 V; $n$ = 45 000 rpm; $\theta_{on} = -7°$; $\theta_{supply} = 90°$ (Fig. 7a)) and $\theta_{supply} = 70°$ (Fig. 7b)). At high rotor speeds, reduction of the supply range from 90° to 70° results in an increase of the produced torque average value because phase currents decay before the dropping inductance zone. When the motor is supplied at its nominal operating point with a supply range of 70°, no negative torque occurs – this can be clearly seen by comparing waveforms of torques $T_{eph1}$ and $T_{eph2}$ in Figs. 7a) and b).

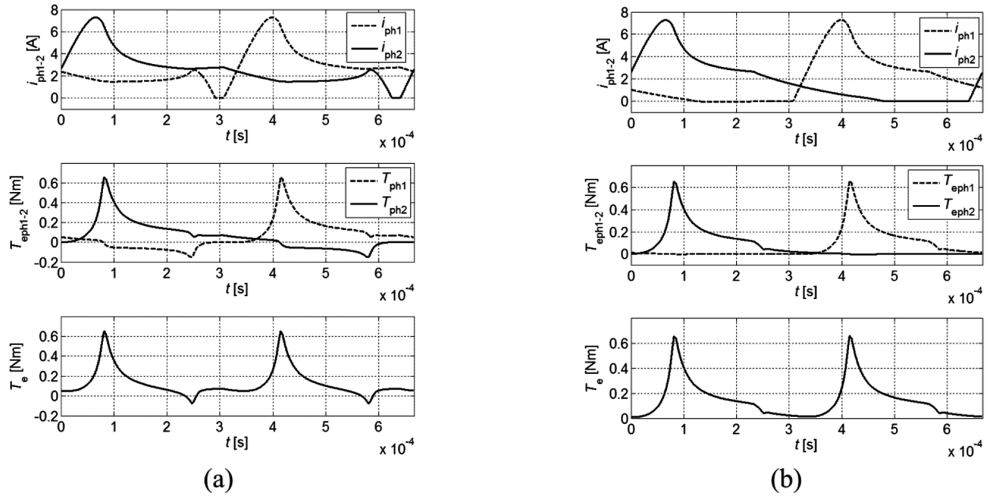


Fig. 7. Waveforms of phase currents $i_{ph1}$, $i_{ph2}$, phase torques $T_{eph1}$, $T_{eph2}$, and total torque $T_e$ for motor speed $n$ = 45 000 rpm, voltage $U_{dc}$ = 325 V, turn-on angle $\theta_{on} = -7°$, and two different supply ranges: a) $\theta_{supply} = 90°$, b) $\theta_{supply} = 70°$

### 4.3. PWM control

In Figure 8, waveforms of phase currents $i_{ph1}$, $i_{ph2}$ and phase voltages $u_{ph1}$, $u_{ph2}$ are shown for two PWM signal carrier wave frequencies $f_{PWM}$ = 8 kHz (Fig. 8a)) and $f_{PWM}$ = 16 kHz (Fig. 8b)) at the duty cycle $\delta$ = 0.8. The waveforms were determined for motor speed $n$ = 39 000 rpm, $U_{dc}$ = 325 V, $\theta_{on} = -3°$, and $\theta_{supply} = 70°$.

It can be seen that at the frequency $f_{PWM}$ = 8 kHz, a significant asymmetry of phase currents appears resulting from too small a ratio of the carrier wave frequency $f_{PWM}$ to the individual phase switching frequency $f_{switch}$. For motor speed $n$ = 39 000 rpm, $f_{switch}$ = 1.3 kHz, and the ratio $f_{PWM}/f_{switch}$ = 6.15. Doubling the frequency $f_{PWM}$ significantly reduces change vari-

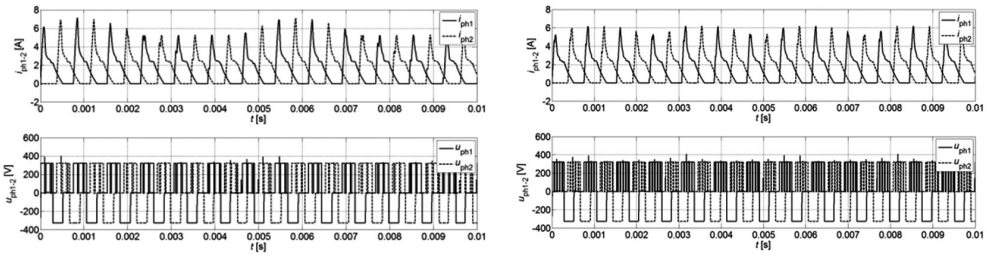


Fig. 8. Waveforms of phase currents ($i_{ph1}$, $i_{ph2}$) and voltages ($u_{ph1}$, $u_{ph2}$) determined for motor speed $n$ = 39 000 rpm and frequencies: a) $f_{PWM}$ = 8 kHz, b) $f_{PWM}$ = 16 kHz

ability of phase current maximum values, although the changes are still clearly visible (Fig. 8b)). When developing a controller for SRM, it should be considered that with increasing switching frequency, losses in power transistor circuits also significantly increase.

### 4.4. Motor starting

In order to simulate the conditions prevailing in the examined machine at starting, the simulation model of Fig. 3 was complemented with the equation of torques (3). To limit the source current at starting, a limitation on the phase current maximum values was introduced. Such a phase current limit has been set to $I_{ref}$ = 10 A. Phase currents and motor speed as functions of time at motor starting are plotted in Fig. 9.

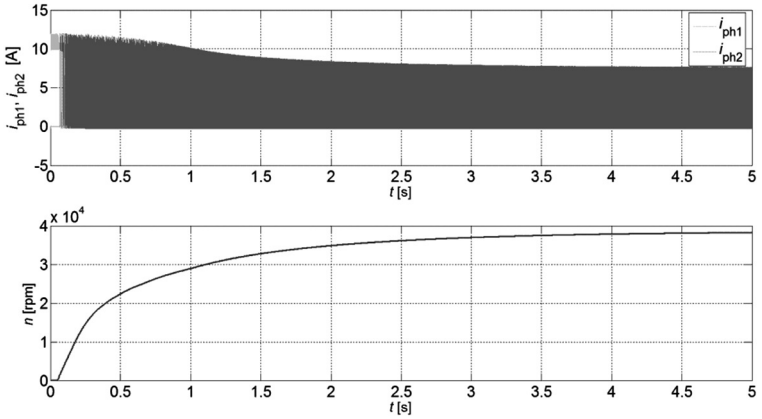


Fig. 9. Phase currents and motor speed as functions of time at the start of two-phase SRM

## 5. Experimental test

Based on results obtained from simulation, a controller for the two-phase SRM was developed and constructed. A view of the controller together with the tested motor is shown in Fig. 10.

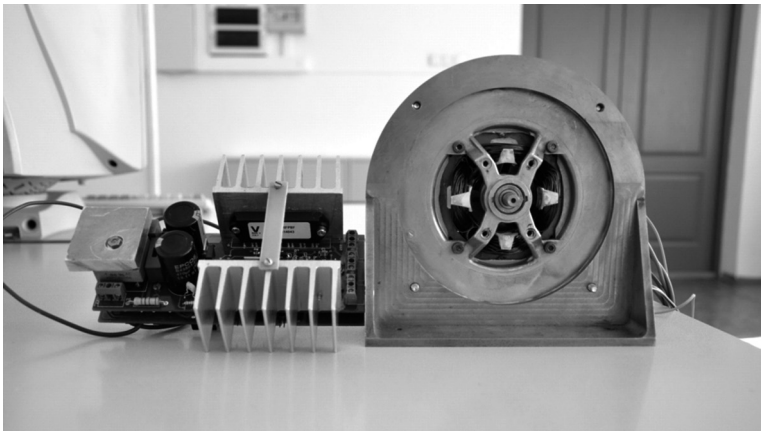

Fig. 10. A view of the 4/2 SRM together with controller

Figs. 11a) and b) present oscillograms registered in the course of the preliminary examination of the motor. The oscillograms were taken at the supply voltage lowered to $U_{dc} = 52$ V.

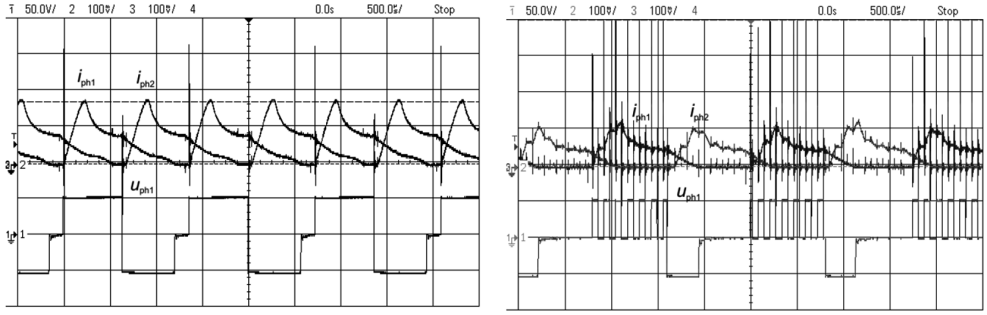


Fig. 11. Phase currents and phase voltage oscillograms for $U_{dc} = 52$ V, $\theta_{on} = -5°$, $\theta_{supply} = 85°$: a) $\delta = 100\%$, $n = 23\,634$ rpm, b) $\delta = 40\%$, $n = 16\,514$ rpm

Figure 11a) shows an oscillogram taken under single-pulse control, while Fig. 11b) presents an oscillogram corresponding to control with the PWM method ($\delta = 40\%$).

## 6. Conclusions

With the use of the mathematical model of the SRM presented above, a simulation model of a high-speed 4/2-pole two-phase SRM with an asymmetric rotor was developed in the MATLAB/Simulink environment. The model was used for carrying out simulations aimed at the determination of performance of the motor at very low rotor speeds (motor starting) as well as at revs close to the nominal speed. The obtained results are expected to be useful in the development of an uncomplicated and inexpensive controller for motors of that type. On the grounds of the obtained results, it can be stated that:

– In the course of motor starting, the supply range should fall into the 90° to 110° bracket in order to ensure sufficient starting torque, whereas the turn-on angle should be properly adapted to the supply range.
– At high rotor speeds, the introduction of speed control by means of a supply voltage with the use of the pulse width modulation method requires the use of a PWM signal carrier wave of high frequency (> 16 kHz); otherwise, a very large asymmetry of phase currents occurs. It must be remembered that an excessively high PWM signal frequency results in significant losses in the converter circuit.
– With PWM control and at high rotor speeds, significant asymmetry of phase currents occurs, therefore, speed control in such circumstances should be exercised by appropriate change of the turn-on angle.

## References

[1] Hamdy R., Fletcher J.E., Williams B.W., *Bidirectional starting of a symmetry two-phase switched reluctance machine*, IEEE Transactions on Energy Conversion, 2000, Vol. 15(2), pp. 211–217.

[2] Wen Ding, Ling Liu, Jianyong Lou, *Design and control of a high-speed switched reluctance machine with conical magnetic bearings for aircraft application*, Electric Power Applications, IET, 2013, Vol. 7(3), pp. 179–190.

[3] Khater M.M., Afifi W.A., Ei-Khazendar M.A., *Operating performances of a two-phase switched reluctance motor*, 11th International Power Systems Conference, MEPCON 2006, Vol. 2, pp. 636–642.

[4] Wróbel K., Tomczewski K., *Jednoczesna optymalizacja kształtu obwodu magnetycznego i parametrów zasilania przełączalnego silnika reluktancyjnego* [*Simultaneous optimization of the magnetic circuit shape and supply parameters of the switched reluctance motor*], Przegląd Elektrotechniczny, 2009, Vol. 85(3), pp. 107–110.

[5] Bogusz P., Korkosz M., Prokop J., *Analiza rozwiązań konstrukcyjnych silników reluktancyjnych przełączalnych przeznaczonych do napędów wysokoobrotowych* [*An analysis of switched reluctance motor solutions designed for high-speed drives*], Zeszyty Problemowe – Maszyny Elektryczne, 2012, No. 1(94), pp. 25–31.

[6] So-Yeon Ahn, Jin-Woo Ahn, Dong-Hee Lee, *A Novel Torque Controller Design for High Speed SRM using Negative Torque Compensator*, IEEE 8th International Conference on Power Electronics and ECCE Asia (ICPE & ECCE), 2011, pp. 937–944.

[7] Qingqing Ma, Daqiang Bi, Baoming Ge, *Digital Control Issue of High Speed Switched Reluctance Motor*, IEEE International Symposium on Industry Electronics (ISIE), 2012, pp. 641–646.